Human Foot Placement and Balance in the Sagittal Plane

Matthew Millard
Derek Wight
John McPhee
Eric Kubica
David Wang

University of Waterloo,
200 University Avenue,
West Waterloo,
ON, N2L 3G1, Canada

*Foot placement has long been recognized as the primary mechanism that humans use to restore balance. Many biomechanists have examined where humans place their feet during gait, perturbations, and athletic events. Roboticists have also used foot placement as a means of control but with limited success. Recently, Wight et al. (2008, "Introduction of the Foot Placement Estimator: A Dynamic Measure of Balance for Bipedal Robotics," ASME J. Comput. Nonlinear Dyn., **3**, p. 011009) introduced a planar foot placement estimator (FPE) algorithm that will restore balance to a simplified biped that is falling. This study tested the FPE as a candidate function for sagittal plane human-foot-placement (HFP) by recording the kinematics of 14 healthy subjects while they performed ten walking trials at three speeds. The FPE was highly correlated with HFP ($\rho \geq 0.997$) and its accuracy varied linearly from 2.6 cm to −8.3 cm as walking speed increased. A sensitivity analysis revealed that assumption violations of the FPE cannot account for the velocity-dependent changes in FPE-HFP error suggesting that this behavior is volitional.* [DOI: 10.1115/1.4000193]

1 Introduction

Balance control is a multifaceted process that relies on estimating the body's state, generation of a desirable future state, the means to make the transition (through foot-placement, center of pressure manipulation, or some other mechanism) and the physical ability to execute the desired action. Foot placement has been identified as the primary means that humans use to restore balance [1,2]. Foot placement is an important component of balance control because the location of the foot determines the origin and possible directions of the ground reaction force vector, which ultimately serve to balance the body. Wight et al. [3] developed a relationship between foot placement and balance—the foot placement estimator (FPE)—that calculates a foot contact location that will *restore* static stability to a simplified biped that is falling. The aim of the FPE to restore balance makes it well suited for analyzing human gait because humans are unbalanced for 80% of the gait cycle [1]. The aim of this investigation is to determine if the FPE can predict sagittal plane human-foot-placement (HFP) during gait initiation, termination, and level walking.

The biomechanics community has investigated foot placement for many years. Lee et al. [4] observed the high-precision, high-speed, visually-controlled foot placements of elite long jumpers who sprinted at 9 m/s yet placed their take-off foot with an error of only 8 cm. Patla and Vickers [5] extended Lee's research by showing that foot placement is guided by vision, modified by the presence of obstacles [6] and contributes to dynamic balance [1] in everyday activities. Redfern et al. [7] characterized foot placement as a function of velocity and vision. Redfern's work has a limited scope of applicability because it is based on heuristics. Townsend and Seireg [8] developed and tested several foot placement algorithms using a computer simulation of gait. The foot placement models of Townsend and Seireg were never validated using human experiments nor were they derived with the aim of restoring balance.

Balance and foot placement are also primary concerns of roboticists. Robotics researchers have explored machine-learning techniques [9,10], trajectory tracking [11,12], passive swing dynamics [13–15], approximate methods [16], and zero-moment point (ZMP) [17] methods to balance bipedal robots. Little can be learned about human balance using machine-learning techniques because they are based on numerical approximation and curve fitting [9,10]. Trajectory tracking bipeds [11,12,18] have a very fragile sense of balance, which suggests that humans do not use this method. Passive swing dynamics explain how humans might be choosing step lengths as a function of walking velocity [19,20] but cannot be applied to gait initiation and termination. The most popular balance definition is the ZMP [17] that is employed in Honda's bipedal robot Asimo [21]. The ZMP is not well suited for analyzing human gait because it requires that at least one foot remains flat on the floor at all times. Humans rarely have one foot flat on the ground while walking [22].

People might not step on the location calculated by the FPE for a variety of reasons. Wight et al. [3] proved that a simplified biped becomes statically balanced in a single step if it steps directly on the FPE (Fig. 2(*c*)). Subjects might not step on the FPE because they do not behave like the simplified biped. A sensitivity analysis will be used to determine how closely humans behave like the simplified biped of Wight et al. [3]. Subjects also may not step at the FPE location when they do not want to become statically balanced (Fig. 2).

While people may not always step on the FPE when walking, we expect they will place their feet in locations that allow them to stop within a single step. The simplified biped has a fixed contact point (Fig. 1), whereas a human foot has a contact area giving people some flexibility about where they choose to place their feet. The center of pressure (COP) is the closest physical analog to the simplified biped's contact point because, like the contact point, moments of the ground reactions about this location sum to zero. As long as the FPE lies within the contact area of the foot, the subject would be guaranteed of stopping by moving their COP on or ahead of the FPE (Fig. 2(*b*)). We expect that subjects will step ahead of the FPE during walking, allowing them to stop in a single step if they desire.

2 Model

Wight et al. [3] developed the FPE to restore balance to a simplified biped (Fig. 1) because more complicated bipeds—such as humans—have unmanageably large equations of motion. The biped consists of a single body with 3 degrees of freedom (planar translation and rotation) and two infinitely small contact points that represent feet attached to the body with rigid massless links. The FPE will calculate where the biped should place its contact point so that after impact it has just enough kinetic energy to

Contributed by the Bioengineering Division of ASME for publication in the JOURNAL OF BIOMECHANICAL ENGINEERING. Manuscript received September 3, 2008; final manuscript received August 25, 2009; accepted manuscript posted September 10, 2009; published online October 29, 2009. Assoc. Editor: Michael Sacks.

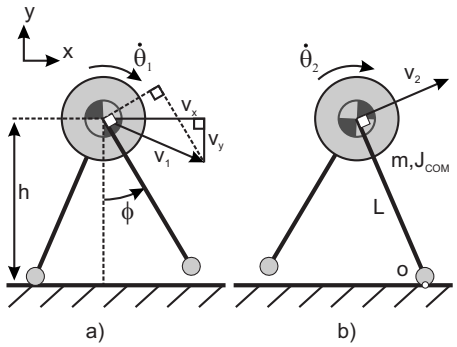

Fig. 1 The simplified biped before and after foot contact, assuming the foot sticks to the ground and momentum is conserved [3]

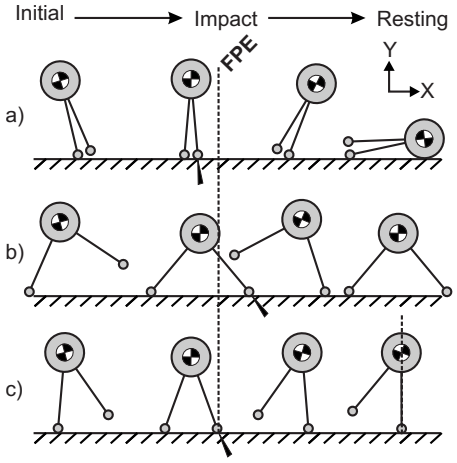

Fig. 2 The simplified biped stepping relative to the FPE [3]: (*a*) stepping closer than the FPE results in falling forward, (*b*) stepping further than the FPE causes the biped to fall back onto the swing leg, and (*c*) stepping precisely at the FPE will balance the COM above the standing foot

transition to a standing position (Fig. 2(*c*)). The derivation for the final expression of the FPE for a simplified biped is shown below. It is assumed that angular momentum is conserved before (Ho_1) and after impact (Ho_2) about the contact point o.

$$Ho_1 = Ho_2 \tag{1}$$

The expression for planar angular momentum (using $s\phi$, $c\phi$ for sin ϕ, and cos ϕ) can be expanded using the biped's mass (m), moment of inertia (J_{COM}) about the center of mass (COM), leg length (L) and its current COM linear (v_x, v_y), and angular ($\dot{\theta}$) speed.

$$mL(v_x c\phi + v_y s\phi) + J_{\mathrm{COM}}\dot{\theta}_1 = (mL^2 + J_{\mathrm{COM}})\dot{\theta}_2 \tag{2}$$

Whole-body average angular speed ($\dot{\theta}_1$ above) is calculated using the equivalent momentum [23] of the tracked body segments.

$$\dot{\theta}_{\mathrm{Avg}} = \frac{\Sigma_{i=1}^{n} J_i \dot{\theta}_i}{\Sigma_{i=1}^{n} J_i} \tag{3}$$

Leg length is described in terms of the current height of the COM to allow for variable leg lengths.

$$L = \frac{h}{c\phi} \tag{4}$$

Defining leg length (L) in this manner means that the FPE can find locations that might not be reachable by a human leg at a given moment in time. The post-impact angular speed of the biped $\dot{\theta}_2$ can be found by substituting Eq. (4) into Eq. (2).

$$\dot{\theta}_2 = \frac{mh(v_x c\phi + v_y s\phi)c\phi + J_{\mathrm{COM}}\dot{\theta}_1 c^2\phi}{mh^2 + J_{\mathrm{COM}}c^2\phi} \tag{5}$$

The FPE is the contact location where the biped's post-contact system energy is equal to its peak potential energy. Peak potential energy is reached when the COM is at its maximum height (h_{peak}) with one contact point still on the ground. System energy refers to the sum of kinetic (T) and potential (V) energy.

$$T_2 + V_2 = mgh_{\mathrm{peak}} \tag{6}$$

Since the simplified biped is in pure rotation after contact, Eq. (6) becomes

$$\tfrac{1}{2}(J_{\mathrm{COM}} + mL^2)\dot{\theta}_2^2 + mgLc\phi = mgL \tag{7}$$

Substituting Eq. (5) into Eq. (7) results in the nonlinear FPE equation to calculate ϕ, the angle at which the leg should be placed.

$$0 = \frac{[mh(v_x c\phi + v_y s\phi)c\phi + J_{\mathrm{COM}}\dot{\theta}_1 c^2\phi]^2}{mh^2 + J_{\mathrm{COM}}c^2\phi} + 2mghc\phi(c\phi - 1) \tag{8}$$

Simple trigonometry can be used to find $X(\phi)$, the location on the floor where the foot should be placed relative to the COM position.

$$X(\phi) = h\tan\phi \tag{9}$$

3 Experimental Methods

Fourteen healthy subjects (seven males and seven females) with a wide range of heights (1.42–1.92 m) and masses (69.5–114.5 kg) were instrumented with OptoTrak IRED markers to track the movements of seven body segments (two feet, shanks, legs, and one lumped head, arms, and trunk (HAT)) in the sagittal plane and record heel contact times while they walked. IRED's were placed on the distal head of the fifth metatarsal (MT), fibular trochlea of the calcaneus (C), the lateral malleolus (LM), the proximal fibular head (FH), the greater trochanter (GT) and the acromion process (AP). Subjects walked with their arms crossed (eliminating the need to track arm movements) for ten trials at 80%, 100%, and 120% of their natural pace using a metronome to cue step timing. Two trial types were recorded: constant cadence walking (Const. walking) and walking that included gait initiation and termination (Init. and term.). Anthropometric tables [22] were used to estimate each of the seven segment masses and inertias (two feet, shanks, legs, and one HAT). The prediction of the FPE was compared with the subject's lateral malleolus location during contact onset. The difference between these two locations ϵ_{LM} was studied using a 2×3 ANOVA (trial type by speed) analysis. Contact was identified kinematically (Sec. 3.1) to allow a larger number of steps to be analyzed than could be done with a limited number of force plates.

At contact onset (t_C), the horizontal location of the lateral malleolus marker ($\boldsymbol{LM}(t_C)\cdot(\hat{x})$) was subtracted from $X(\phi)$ (Eq. (9)) to obtain the FPE-HFP error (ϵ_{LM}). Similarly, the flat-footed horizontal location of the fifth metatarsal ($\boldsymbol{MT}(t_C)\cdot(\hat{x})$) was subtracted from the FPE (forming ϵ_{MT}) to determine if the FPE was ahead of the foot's contact area. These differences are shown in Eq. (10), where the letter "A" has been used to replace marker identifiers LM and MT.

$$\epsilon_A = X(\phi(t_C)) - \boldsymbol{A}(t_C)\cdot\hat{x} \tag{10}$$

The lateral malleolus was chosen as the reference point for analysis because of its ease of identification across subjects. Contact onset was used because it allowed the simultaneous measurement of human foot placement and the body's state before it was affected by ground reaction forces.

3.1 Kinematically Identifying Contact Onset. Accurately measuring the time of contact onset using foot kinematics was challenging. Thresholding the height of the foot can only identify contact with an accuracy of 100 ms [24], which is too crude for the present study. Ground reaction forces develop very quickly during heel contact and affect the velocity of the foot. Different velocity signatures of contact onset were investigated: The vertical and horizontal speeds of the three markers on the foot and the foot's angular velocity.

Contact onset was identified using a combination of thresholding and velocity signature analysis. Heel-first contacts caused the horizontal speed of the LM marker to increase when the heel gripped the ground and pitched the foot forward. Unfortunately, two subjects often contacted the ground flat-footed, eliminating the LM velocity signature. Flat-footed contacts could be identified, however, by the large differences in the contact times estimated by the thresholding method [24] and the LM velocity signature. These two methods were used to measure foot contact time with a high temporal resolution and ignore steps where they disagreed.

A trial was collected with both kinematic and force plate data to validate the foot contact identification algorithm. The force plate measured the true time of contact onset when its vertical load exceeded twice the standard deviation (σ=2.11 N) of the plate's resting noise. The kinematic contact time lagged the force plate's estimate by 0–10 ms at which time the load on the plate was 2.86–16.3 N. The effect of the delay on the FPE-HFP error was estimated by multiplying the FPE-HFP velocity ($d\mathrm{LM}_x/dt - dX(\phi)/dt$) by the maximum 10 ms time lag.

3.2 Validation of Assumptions. FPE assumption violations were quantified using a sensitivity analysis. The FPE makes four assumptions: that momentum is conserved during contact and that the leg length, moment of inertia, and system energy (the sum of kinetic and potential energy) are constant. Since the FPE is continuously differentiable it is possible to take partial derivatives of $X(\phi)$ at the time of foot contact. The change in angular momentum (ΔHo), leg length (ΔL), moment of inertia (ΔJ_{COM}), and kinetic and potential energy sum ($\Delta(T+V)$) was calculated between foot contact and the time the COM passes over the lateral malleolus (Fig. 4)—the moment when the simplified biped of Wight et al. [3] comes to rest when it steps on the FPE. The error of the FPE due to the observed violations was estimated by taking the product of the partial derivatives and the observed differences.

Examining the assumption that angular momentum is conserved during heel strike is difficult because the simplified biped has a fixed contact point whereas the human foot has a moving contact area. The COP could be analyzed because it is the closest physical analog to the simplified biped's contact point. Calculating angular momentum about the COP (Eq. (11)) produces misleading results because its movement has a dramatic effect on the angular momentum profile.

$$\boldsymbol{Ho}_{\mathrm{ref}}(t) = \sum_{i=1}^{7} J_i\boldsymbol{\omega}_i(t) + (\boldsymbol{r}_i(t) - \boldsymbol{r}_{\mathrm{COP}}) \times m_i(\boldsymbol{v}_i(t) - \boldsymbol{v}_{\mathrm{COP}}(t)) \tag{11}$$

Since the magnitude of the $J_i\omega_i$ terms of the body's angular momentum are minimal [25], the cross product terms $(\boldsymbol{r}_i - \boldsymbol{r}_{\mathrm{COP}}) \times m(\boldsymbol{v}_i - \boldsymbol{v}_{\mathrm{COP}})$ dominate. In early stance the COP moves forward quickly, making the $(\boldsymbol{v}_i - \boldsymbol{v}_{\mathrm{COP}})$ term small, resulting in small angular momentum values. The COP slows down in midstance making the cross product terms significantly larger, increasing the calculated angular momentum. The large variation in angular momentum is misleading because it is being caused by the movement of the COP rather than the contact event.

A fixed point of reference is required to determine if angular momentum is conserved during foot contact. The ground projection of the LM at mid stance (when the COM is over the LM) was chosen as a reference point. This location was chosen because it approximates the COP's final location if the person stopped as the simplified biped does. Whole-body angular momentum was calculated by summing the angular momentum of each segment about its own COM ($J_i\boldsymbol{\omega}_i$) and then about the reference point $(\boldsymbol{r}_i - \boldsymbol{r}_{\mathrm{LMGP}}) \times m_i(\boldsymbol{v}_i)$ as in Eq. (12).

$$\boldsymbol{H}_{\mathrm{LMGP}}(t) = \sum_{i=1}^{7} J_i\boldsymbol{\omega}_i(t) + (\boldsymbol{r}_i(t) - \boldsymbol{r}_{\mathrm{LMGP}}) \times m_i(\boldsymbol{v}_i(t)) \tag{12}$$

Leg length was measured using the Euclidean distance between the whole-body COM and the LM of the contacting foot to be consistent with the FPE of Wight et al. [3]

$$L(t) = |\boldsymbol{r}_{\mathrm{COM}}(t) - \boldsymbol{r}_{\mathrm{LM}}(t)| \tag{13}$$

The moment of inertia of the body was calculated about the body's COM using the following equation:

$$J(t)_{\mathrm{COM}} = \sum_{i=1}^{7} J_i + m_i|\boldsymbol{r}_i(t) - \boldsymbol{r}_{\mathrm{COM}}(t)|^2 \tag{14}$$

The sum of kinetic and potential energy was calculated for each segment as

$$T(t) + V(t) = \sum_{i=1}^{7} \frac{1}{2}m_i|\vec{v}_i(t)|^2 + \frac{1}{2}J_i|\vec{\omega}_i(t)|^2 + m_i g h_i(t) \tag{15}$$

Changes in each of these quantities (ΔA), except angular momentum (Ho), were calculated by taking the maximum difference that occurred between foot contact and the time the body's COM passed over the lead ankle.

$$\Delta A = \max(A(t)) - \min(A(t)) \tag{16}$$

Unlike the changes in the quantities listed above, the change in angular momentum (ΔH_{LMGP}) was calculated by taking a local maximum difference using its value at contact onset ($H_{\mathrm{LMGP}}(t_C)$) as a reference. Contact onset must be used as a reference because the model assumes that angular momentum is conserved during contact. After contact, angular momentum is free to vary, and in the case of the model decreases to zero when the biped becomes balanced.

Since the FPE equation is implicit, the required differentials were calculated numerically at the time of foot contact

$$\frac{\partial X(\phi)}{\partial H_{\mathrm{LMGP}}} \approx \frac{X(\phi,(1+\delta)H_{\mathrm{LMGP}}) - X(\phi,H_{\mathrm{LMGP}})}{\delta H_{\mathrm{LMGP}}} \tag{17}$$

$$\frac{\partial X(\phi)}{\partial J_{\mathrm{COM}}} \approx \frac{X(\phi,(1+\delta)J_{\mathrm{COM}}) - X(\phi,J_{\mathrm{COM}})}{\delta J_{\mathrm{COM}}} \tag{18}$$

$$\frac{\partial X(\phi)}{\partial L} \approx \frac{X(\phi,(1+\delta)L) - X(\phi,L)}{\delta L} \tag{19}$$

$$\frac{\partial X(\phi)}{\partial (T+V)} \approx \frac{X(\phi,(1+\delta)(T+V)) - X(\phi,(T+V))}{\delta (T+V)} \tag{20}$$

Each partial derivative was assessed for numerical stability by calculating the relative error between each partial using progressively smaller values of δ (0.01, 0.001, and 0.0001). The largest discrepancy between any of the partial derivatives was a mere 0.37% indicating that an appropriately small value of δ had been chosen for each partial derivative.

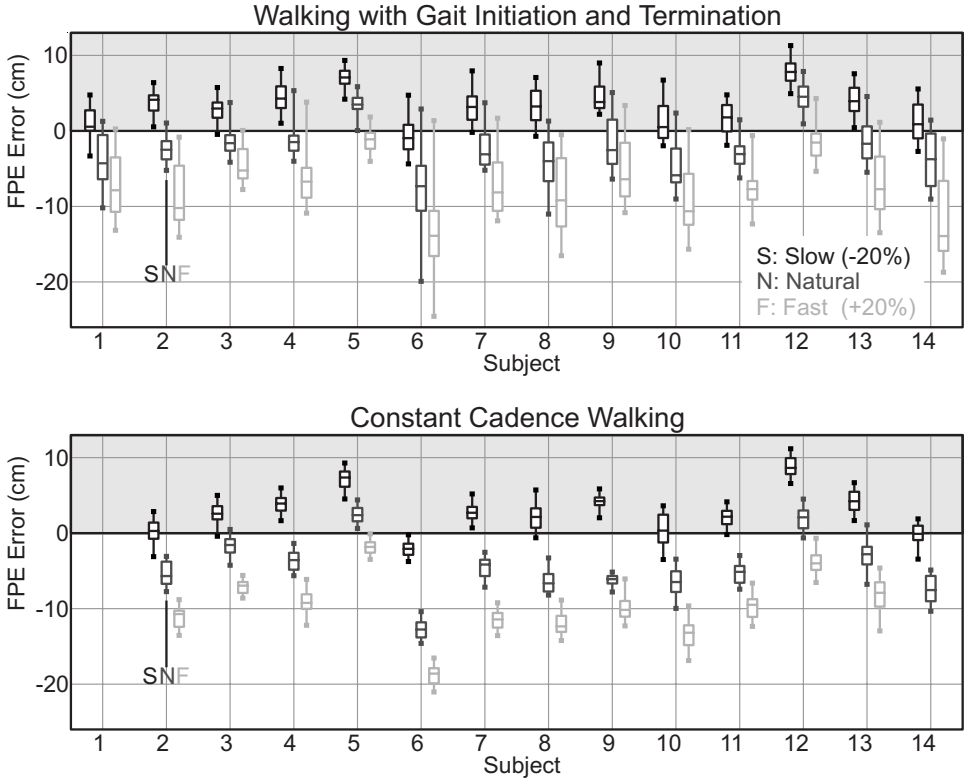

Fig. 3 Box and whisker plots of the error between the FPE and each subject's lateral malleolus at foot contact. Whiskers run between the fifth and the 95th percentiles; boxes between the 25th and the 75th percentiles with a hash at the 50th percentile. Natural paced trials align with the subject number; slow trials are immediately to the left and fast trials are to the right. Subjects are motivated by not only balance but pace and acceleration since they step further behind the FPE as they walk faster and with more variation when they initiate and terminate gait. We failed to collect constant cadence trials for subject 1, and fast constant cadence trials for subject 14.

4 Results

The 4257 steps recorded in this study are highly correlated with the predictions of the FPE ($\rho \geq 0.997$ in Table 1) and so an ANOVA was used to study the differences in detail. The ϵ_{LM} data were analyzed with a 2×3 (trial type by speed) repeated measures ANOVA, which found significant main effects for speed ($F(24,200)=4659.03$, $p<0.0001$) and trial type ($F(14,200)=529.98$, $p<0.0001$). The FPE-HFP error varied systematically for different walking speeds (Fig. 3). The FPE-HFP error was also significantly different in trials that included gait initiation and termination compared with constant cadence trials (Fig. 3). In addition, the standard deviation of the FPE-HFP error σ_{LM} is much smaller than the stride length standard deviation, σ_{SL} (Table 1), suggesting that the model is successfully capturing the important dynamics of the foot placement process. The analysis also showed significant interactions between subject and pace ($F(264,200)=11.45$, $p<0.0001$), subject and trial type ($F(124,200)=10.25$, $p<0.0001$), and trial type and speed ($F(24,200)=75.09$, $p<0.0001$). These interactions offer little information because the trial type by speed interaction was expected and the subject interactions are due to individual differences. The data do not satisfy the ANOVA's assumptions because only 49 out of 80 of the FPE-HFP error distributions are normal (using Kolmogorov–Smirnov, Cramer–Von Mises, and Anderson–Darling tests), and the variances are not equal (using Levene's test). The findings should be unaffected by these assumption violations because the differences are so strong and a repeated measures ANOVA is robust against such errors [26]. We failed to collect constant cadence walking trials for subject 1, and fast constant cadence walking trials for subject 14. If the data of subject 1 and 14 are excluded from the data set the F-values increase by 2–10% yet the findings remain unchanged. We chose to include the data of subject 1 and 14 in the analysis.

Table 1 The FPE and HFP are highly correlated (ρ). The FPE-HFP error means $\mu(\epsilon_{LM})$ and standard deviations $\sigma(\epsilon_{LM})$ change systematically with trial type and pace. The FPE is capturing the important dynamics of HFP since the FPE-HFP error standard deviations $\sigma(\epsilon_{LM})$ are much smaller than the stride length standard deviations σ_{SL}. The mean $\mu(\epsilon_{MT})$ and standard deviation $\sigma(\epsilon_{MT})$ of the distance between the FPE and the flat-footed position of the MT marker ϵ_{MT} indicate that subjects place their MT ahead of the FPE, allowing them to stop in a single step if desired. All quantities except ρ are in units of cm.

	Init. and term.			Const. walking		
	Slow	Nat.	Fast	Slow	Nat.	Fast
ρ	0.999	0.999	0.999	0.997	0.997	0.998
$\mu(\epsilon_{LM})$	3.27	−2.02	−6.85	2.57	−4.12	−8.28
$\sigma(\epsilon_{LM})$	2.40	3.18	4.43	1.60	1.50	1.45
σ_{SL}	7.36	10.5	17.6	2.96	2.73	2.15
$\mu(\epsilon_{MT})$	16.2	10.8	5.72	16.2	8.85	3.55
$\sigma(\epsilon_{MT})$	2.57	3.34	4.54	1.92	1.64	1.80

Despite the strong trial and subject dependent FPE-HFP error differences, subjects appear to place the leading edge of their foot *ahead* of the FPE during natural and slower paced walks (see

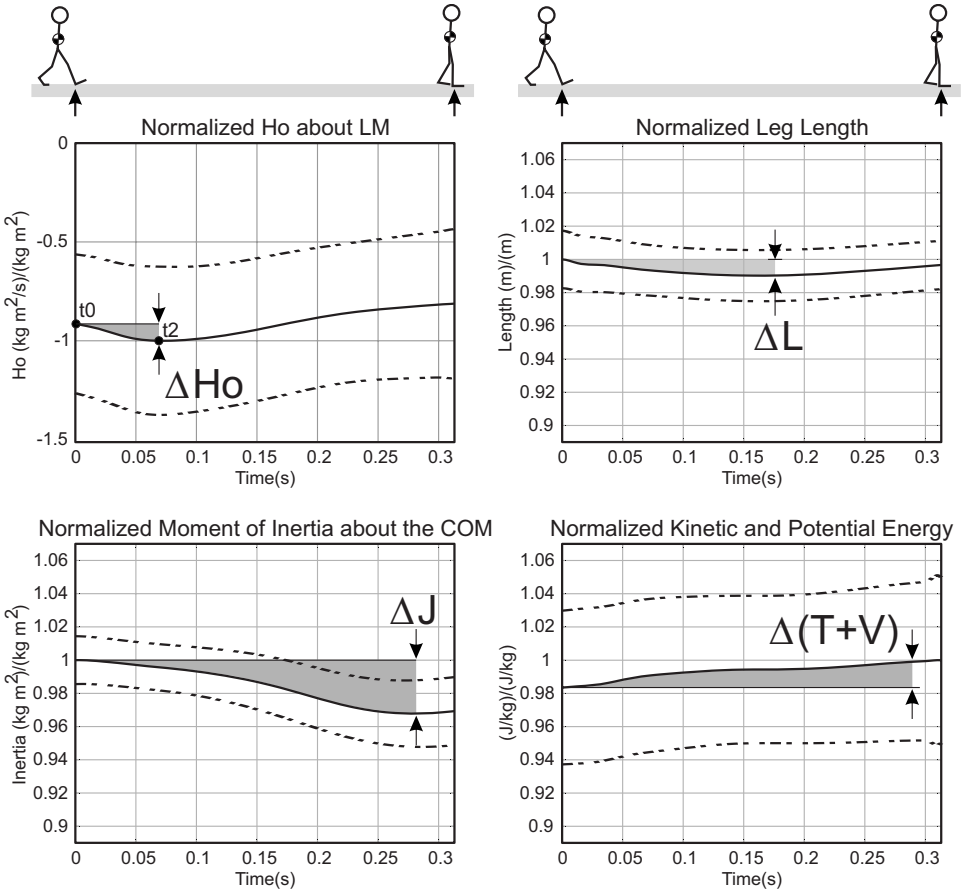

Fig. 4 Group ensemble plots of dimensionless normalized *Ho*, *L*, *J*, and *T+V* profiles between heel strike and the moment the COM passes over the LM. Means are drawn with a solid line while ±1 standard deviation is shown with a dotted line. The natural paced constant cadence trial is shown. The assumption that angular momentum is conserved is violated since it increases. The assumptions of constant *L*, *J*, and *T+V* are reasonable. Note that the sum of kinetic and potential energy (*T+V*) plot does not change appreciably because potential energy (*V*) dominates and remains relatively constant.

$\mu(\epsilon_{MT})$ and $\sigma(\epsilon_{MT})$ in Table 1), allowing them to stop without taking an extra step. Only 212 of the 4257 steps analyzed had the MT behind the FPE, with nearly half (95) generated by subject 6 whose natural cadence was a brisk 112 steps per min, far faster than the rest of the subjects (100 ± 7.71 steps per min). The remaining exceptional steps were generated by other subjects during the fast paced trials (111), with very few occurring in natural paced trials (4).

The velocity-dependent changes of the FPE-HFP error could be caused by a systematic violation of the assumptions of the FPE as described in Sec. 3. Most of the assumptions of the model of Wight et al. [3] are met (Fig. 4) and affect the FPE calculation and the FPE-HFP error very little (Table 2). In addition, the temporal error of the kinematic contact estimation technique could have affected the results only by 3.6 ± 0.6 mm (Table 2). The assumption that angular momentum (***Ho***) is conserved during contact is broken; angular momentum actually increases due to a coordinated weight acceptance and push-off phase [27]. When the extra momentum is taken into account, the FPE predicts that the subjects should have stepped 2–3 cm further ahead (Tables 2 and 3), when in reality they stepped further behind the FPE as they walked faster. Based on the data and the analysis of the model's assumptions we suggest that the velocity-dependent FPE-HFP error is volitional rather than being the result of a systematic violation of the FPE assumptions.

5 Discussion

The simplified biped used by the FPE serves as a useful tool to interpret the functional relevance of the unmodeled velocity and acceleration adjustments that subjects appear to be making. Subjects stepped further behind the FPE as they walked faster (Fig. 3). Stepping a constant distance behind the FPE would allow the simplified biped, and thus the person, to maintain a set forward speed rather than stopping (Fig. 2). Similarly, stepping further and further behind (ahead) the FPE on each step would cause the simplified biped to accelerate (decelerate) explaining the increased variation in trials with gait initiation and termination.

Individual differences are evident in the significant subject by pace ($p < 0.0001$), and subject by trial type ($p < 0.0001$) interactions. Most subjects step behind the FPE on average whereas subjects 5 and 6 step ahead; $\sigma(\epsilon_{LM})$ of subjects 3, 5, 11, and 12 hardly changes between continuous walking and trials with gait initiation and termination, whereas it increases appreciably for other subjects. The simplified biped of Wight et al. [3] would suggest that those who on average step ahead of the FPE walk conservatively because they are guaranteed of being able to stop within a single step (Fig. 2). Subject-specific biases can also be explained with anthropometric parameter errors. The FPE calculation is dependent on an accurate calculation of whole-body angular momentum. The cross product term $((\boldsymbol{r}(t)_i - \boldsymbol{r}(t)_{LMGP}) \times m_i \boldsymbol{v}(t)_i)$ of the

Table 2 The sensitivity analysis summary statistics indicate that violating the assumption of conservation of momentum could affect the FPE calculation by 2.18 cm on average, which cannot account for the observed −2.2 cm FPE-HFP error. The assumptions of constant leg length, inertia, and system energy are quite good as the observed changes would only influence the FPE-HFP error on the order of millimeters or less. All quantities in the final column are in units of cm.

W	$\frac{\partial X(\phi)}{\partial W} \pm \sigma$	$\Delta W \pm \sigma$	$\frac{\partial X(\phi)}{\partial W}\Delta W \pm \sigma$
Ho	0.27 ± 0.0046	7.31 ± 2.3	2.18 ± 0.64
J	-0.10 ± 0.0056	0.45 ± 0.036	-0.050 ± 0.0054
L	-0.077 ± 0.47	1.12 ± 0.13	-0.11 ± 0.016
$T+V$	$1.25 \times 10^{-4} \pm 7.49 \times 10^{-6}$	15.33 ± 7.25	0.21 ± 0.097
$\frac{d\epsilon_{\mathrm{LM}}}{dt}$	-35.6 ± 5.52 cm/s	$\Delta t_{\max} 0.010$	-0.36 ± 0.06
		$\Delta \epsilon_{\mathrm{LM}} \pm \sigma$	-2.20 ± 0.96

Table 3 Linear approximation of the effect of the velocity-dependent violation of ΔH_{LMGP} on $X(\phi)$. Although the magnitudes are similar to the observed error between $\Delta X(\phi)$ and human foot placement, in almost all cases the systematic violation of the conservation of momentum assumption would make the FPE-HFP error larger than observed. Thus the observed systematic change in FPE-HFP error is likely volitional rather than due to a violation of the model's assumptions. The final column is in units of cm.

Init. and term.	Slow: −20%	Natural	Fast: 20%
$\frac{\epsilon_{\mathrm{LM}}}{\delta H_{\mathrm{LMGP}}}\Delta H_{\mathrm{LMGP}}$	2.77 ± 1.03	2.68 ± 1.29	2.62 ± 1.55
ϵ_{LM}	3.27 ± 2.40	-2.02 ± 3.18	-6.85 ± 4.43
Const. walking	Slow: −20%	Natural	Fast: 20%
$\frac{\delta X(\phi)}{\delta H_{\mathrm{LMGP}}}\Delta H_{\mathrm{LMGP}}$	2.85 ± 0.62	2.70 ± 0.87	2.67 ± 1.04
ϵ_{LM}	2.57 ± 1.60	-4.12 ± 1.50	-8.28 ± 1.45

HAT segment makes up $83.6\% \pm 1.03\%$ of the whole-body angular momentum (across all subjects and trials), making it important to estimate each subject's HAT mass accurately. The FPE calculation would change by 2–3 cm for a plausible 10% error [28] in the estimate of the HAT's mass. This error is large enough to account for some subject-specific biases but not all. Accurate means to measure or estimate subject segment masses are needed to interpret the observed subject-specific FPE-HFP biases.

6 Conclusions

A mathematical understanding of the mechanics of balance control in humans is highly desirable for both its potential diagnostic and rehabilitation applications. Foot placement has long been recognized as a critical component of the human balance system yet relatively little work has been done to find and validate mathematical models to describe this relationship. The FPE of Wight et al. [3] is unique in that it was derived with the sole goal of balancing a simplified biped. Importantly, this work has shown that the vast majority of a human step is described by the FPE and that the differences that do exist are due to an unmodeled adjustment people are making in an effort to maintain velocity or to accelerate through the stance phase. In addition, during slow and naturally paced gaits, subjects place the leading edge of their foot ahead of the FPE allowing them to stop without taking an extra step if they desire. Subject-specific differences exist and can be explained using human behavior or anthropomorphic parameter errors. Better means of estimating segment inertial properties are needed before these subject-specific differences can be interpreted properly. This model has great potential to illuminate many areas of gait ranging from quantifying bipedal instability and balance performance, identifying people with compromised balance, and improving forward dynamic gait simulations. It is our hope that this work will motivate further human balance research and that its application will lead to a reduction in fall-related injuries.

7 Future Work

The most important applications of the FPE lie in quantifying instability and evaluating balance performance. Provided the assumptions of the FPE are met, the distance between the FPE location and the biped's COM is a direct measure of instability. The location of the subject's COM, their foot contact location, and the FPE can be used to quantify how effective the step was at restoring balance. Instability and balance performance measures will be highly useful for understanding bipedal balance and how it can fail.

Existing balance measures are either too restrictive or too limited to quantify instability and balance performance accurately for large perturbations. Many attempts have been made to quantify human stability using heuristic metrics [29–31] and more recently by examining orbital and local stability measures [29,32]. Heuristic balance metrics are difficult to use because the regions of stability and validity have not been formally established, nor are they accompanied by a stability proof. Orbital stability measures are limited because they can only be applied to periodic motions; aperiodic motions such as compensatory stepping, gait initiation, and termination cannot be analyzed. Local stability measures can be used for aperiodic motion but only for small perturbations away from a periodic motion. An extension of the FPE theory will allow bipedal responses to small and large perturbations to be studied in detail without restrictive assumptions.

Theoretical and experimental work needs to be completed to realize the full benefits of the FPE. A 3D version of the FPE, complete with stability proofs, regions of stability and validity, needs to be developed as Wight et al. [3] did in 2D. The details of how best to formulate instability and balance performance using the FPE require theoretical development and experimental validation. Compensatory stepping experiments with 3D perturbations need to be completed to compare the 3D FPE derived measures for instability and balance restoration to existing measures. Perturbation experiments using different population groups will need to be completed to determine if these new measures would be useful diagnostic tools. Work has begun to extend the FPE to 3D, which will be presented in a companion paper.

Acknowledgment

This research was supported by the Natural Sciences and Engineering Research Council of Canada. Michael MacLellan, Jeremy Noble, and Heather Lillico generously donated their time to help with the data collection. We are grateful to the University of Waterloo's Kinesiology Department for giving us access to their laboratories for the experimental phase of this study. Professor Paul Calamai provided very helpful advice on validating numerical partial derivatives used in the sensitivity analysis.

Nomenclature

COM = center of mass
FPE = foot placement estimator

HFP = human foot placement location
FPE-HFP Error = distance between the FPE and the HFP
ϵ_{LM} = horizontal distance between the FPE and LM during contact onset (cm)
ϵ_{MT} = horizontal distance between the FPE and MT (when foot is flat) during contact onset (cm)
HAT = head arms and trunk segment
MT = distal 5th metatarsal head
C = Fibular trochlea of the calcaneus
LM = lateral malleolus
FH = proximal fibular head
GT = greater trochanter
AP = acromion process
μ = average
σ = standard deviation
ρ = correlation coefficient
g = the acceleration due to gravity (9.81 m/s^2)
h = COM height (m)
h_{peak} = peak height the COM can reach with 1 foot on the ground (m)
Ho_1 = angular momentum about contact point o, prior to contact (kg m^2/s)
Ho_2 = angular momentum about contact point o, after contact (kg m^2/s)
H_{LMGP} = angular momentum about the ground projection of the LM (kg m^2/s)
J_{COM} = moment of inertia about the COM (kg m^2)
J_i = inertia of the ith segment (kg m^2)
m = mass (kg)
m_i = mass of the ith segment (kg)
L = leg length (m)
$\boldsymbol{r}_i$ = vector to the COM of the ith segment (m)
$\boldsymbol{r}_{COM}$ = vector to the entire body's COM (m)
$\boldsymbol{r}_{LM}$ = vector to the LM (m)
$\boldsymbol{r}_{LMGP}$ = vector to the LM ground projection (m)
T = kinetic energy of the body (J)
$T+V$ = system energy (J)
t_C = time of contact onset (s)
V = potential energy of the body (J)
$\boldsymbol{v}(t)_i$ = linear velocity of the COM of the ith segment (m/s)
v_x = X component of the precontact COM velocity (m/s)
v_y = Y component of the precontact COM velocity (m/s)
$X(\phi)$ = the location of the FPE on the floor (m)
ϕ = angle between the vertical and the lead leg (rad)
$s\phi$ = $\sin(\phi)$
$c\phi$ = $\cos(\phi)$
$\frac{\partial X(\phi)}{\partial H_{LMGP}}$ = rate of change in $X(\phi)$ with respect to H_{LMGP} ($m/[kg\ m^2/s]$)
$\frac{\partial X(\phi)}{\partial J_{COM}}$ = rate of change in $X(\phi)$ with respect to J_{COM} ($m/[kg\ m^2]$)
$\frac{\partial X(\phi)}{\partial L}$ = rate of change in $X(\phi)$ with respect to L (m/m)
$\frac{\partial X(\phi)}{\partial (T+L)}$ = rate of change in $X(\phi)$ with respect to $T+L$ (m/J)
$\boldsymbol{\omega}_i$ = angular velocity of the ith segment about its COM (rad/s)
$\dot{\theta}_1$ = angular speed of the body before contact (rad/s)
$\dot{\theta}_2$ = angular speed of the body after contact (rad/s)

References

[1] Patla, A., 2003, "Strategies for Dynamic Stability During Adaptive Human Locomotion," IEEE Eng. Med. Biol. Mag., **22**, pp. 48–52.
[2] Patla, A., Wijneberg, N., and Hill, S., 1999, "Control of COM by COP Explains the Response Reversal Observed During Medio-Lateral Perturbations Applied During Human Locomotion," Gait Posture, **9**, p. S4.
[3] Wight, D., Kubica, E., and Wang, D., 2008, "Introduction of the Foot Placement Estimator: A Dynamic Measure of Balance for Bipedal Robotics," ASME J. Comput. Nonlinear Dyn., **3**, p. 011009.
[4] Lee, D., Lishman, J., and Thomson, J., 1982, "Regulation of Gait in Long Jumping," J. Exp. Psychol. Hum. Percept. Perform, **8**, pp. 448–459.
[5] Patla, A., and Vickers, J., 2003, "How Far Ahead Do We Look When Required to Step on Specific Locations in the Travel Path During Locomotion," Exp. Brain Res., **148**, pp. 133–138.
[6] Patla, A., Prentice, S., Reitdyk, S., Allard, F., and Martin, C., 1999, "What Guides the Selection of Alternate Foot Placement During Locomotion in Humans," Exp. Brain Res., **128**, pp. 441–450.
[7] Redfern, M., and Schumann, T., 1994, "A Model of Foot Placement During Gait," J. Biomech., **27**, pp. 1339–1346.
[8] Townsend, M., and Seireg, A., 1972, "The Synthesis of Bipedal Locomotion," J. Biomech., **5**, pp. 71–83.
[9] Juang, J–G., 2000, "Fuzzy Neural Network Approaches for Robotic Gait Synthesis," IEEE Trans. Syst., Man, Cybern., Part B: Cybern., **30**(4), pp. 594–601.
[10] Taga, G., Yamaguchi, Y., and Shimizu, H., 1991, "Self-Organized Control of Bipedal Locomotion by Neural Oscillators in Unpredictable Environment," Biol. Cybern., **65**, pp. 147–159.
[11] Wojtyra, M., 2003, "Multibody Simulation Model of Human Walking," Mech. Based Des. Struct. Mach., **31**(3), pp. 357–377.
[12] Peasgood, M., Kubica, E., and McPhee, J., 2007, "Stabilization and Energy Optimization of a Dynamic Walking Gait Simulation," ASME J. Comput. Nonlinear Dyn., **2**, pp. 65–72.
[13] Pratt, J., and Pratt, G., 1999, "Exploiting Natural Dynamics in the Control of a 3D Bipedal Walking Simulation," CLAWAR, Portsmouth, UK.
[14] Kuo, A., 2002, "Energetics of Actively Powered Locomotion Using the Simplest Walking Model," ASME J. Biomech. Eng., **124**, pp. 113–120.
[15] McGeer, T., 1993, "Dynamics and Control of Bipedal Locomotion," J. Theor. Biol., **163**, pp. 277–314.
[16] Raibert, M., 1986, *Legged Robots That Balance*, 1st ed., MIT, Cambridge, MA.
[17] Vukobratovic, M., and Barovac, B., 2004, "Zero-Moment Point—Thirty Five Years of Its Life," J. Humanoid Rob., **1**(1), pp. 157–173.
[18] Millard, M., McPhee, J., and Kubica, E., 2009, "Multi-Step Forward Dynamic Gait Simulation," *Multibody Dynamics: Computational Methods and Applications*, C. Bottasso, ed., Springer, New York, pp. 25–43.
[19] Kuo, A., 2001, "A Simple Model of Bipedal Walking Predicts the Preferred Speed-Step Length Relationship," ASME J. Biomech. Eng., **123**, pp. 264–269.
[20] Whittlesey, S., Van Emmerik, R., and Hamill, J., 2000, "The Swing Phase of Human Walking is Not a Passive Movement," Motor Control, **4**, pp. 273–292.
[21] Hirai, K., Hirose, M., Haikawa, Y., and Takenaka, T., 1998, *The Development of Honda Humanoid Robot*, ICRA.
[22] Winter, D., 2005, *Biomechanics and Motor Control of Human Movement*, 3rd ed., Wiley, Hoboken, NJ.
[23] Essen, H., 1993, "Average Angular Velocity," Eur. J. Phys., **14**, pp. 440–445.
[24] Karcnik, T., 2003, "Using Motion Analysis Data for Foot-Floor Contact Detection," Med. Biol. Eng. Comput., **41**, pp. 509–512.
[25] Herr, H., and Popovic, M., 2008, "Angular Momentum in Human Walking," J. Exp. Biol., **211**, pp. 467–481.
[26] Riffenburgh, R., 2006, *Statistics in Medicine*, 2nd ed., Elsevier, Burlington, MA.
[27] Donelan, J., Kram, R., and Kuo, A., 2002, "Simultaneous Positive and Negative External Mechanical Work in Human Walking," J. Biomech., **35**, pp. 117–124.
[28] Kingma, I., Toussaint, H., De Looze, M., and Van Dieen, J., 1996, "Segment Inertial Parameter Evaluation in Two Anthropomorphic Models by Application of a Dynamic Linked Segment Model," J. Biomech., **29**, pp. 693–704.
[29] Hurmuzlu, Y., and Basdogan, C., 1994, "On the Measurement of Dynamic Stability of Human Locomotion," ASME J. Biomech. Eng., **116**, pp. 30–36.
[30] Hof, A., Gazendam, M., and Sinke, W., 2005, "The Condition for Dynamic Stability," J. Biomech., **38**(1), pp. 1–8.
[31] Karcnik, T., 2004, "Stability in Legged Locomotion," Biol. Cybern., **90**, pp. 51–58.
[32] Dingwell, J., and Kang, H., 2007, "Differences Between Local and Orbital Dynamic Stability During Human Walking," ASME J. Biomech. Eng., **129**, pp. 586–593.